Du et al. Nanoscale Research Letters (2015) 10:321
DOI 10.1186/s11671-015-1030-0

Nanoscale Research Letters
a SpringerOpen Journal

NANO EXPRESS Open Access

Enhanced Photovoltaic Performance of Dye-Sensitized Solar Cells by Efficient Near-Infrared Sunlight Harvesting using Upconverting $Y_2O_3:Er^{3+}/Yb^{3+}$ Phosphor Nanoparticles

Peng Du, Joo Ho Lim, Jung Woo Leem, Sung Min Cha and Jae Su Yu*

Abstract

We report the efficiency enhancement in dye-sensitized solar cells (DSSCs) using Er^{3+}/Yb^{3+}-co-doped Y_2O_3 (i.e., $Y_2O_3:Er^{3+}/Yb^{3+}$) phosphor nanoparticles, prepared by a simple and cost-effective urea-based homogeneous precipitation method, for efficient near-infrared (NIR) sunlight harvesting. Under the light excitation at a wavelength of 980 nm, the as-prepared samples exhibited strong upconversion emissions at green and red visible wavelengths. To investigate the influence of $Y_2O_3:Er^{3+}/Yb^{3+}$ nanoparticles on the photovoltaic performance of DSSCs, the phosphor nanoparticles were incorporated into titanium dioxide films to form a composite photoelectrode. For the resulting DSSCs, the increased power conversion efficiency (*PCE*) of 6.68 % was obtained mainly by the increased photocurrent of $J_{SC} = 13.68$ mA/cm^2 due to the light harvesting enhancement via the NIR-to-visible upconversion process (cf., $PCE = 5.94$ %, $J_{SC} = 12.74$ mA/cm^2 for the reference DSSCs without phosphor nanoparticles), thus, indicating the *PCE* increment ratio of ~12.4 %.

Keywords: Upconversion; Rare-earth; Luminescence; Dye-sensitized solar cells

Background

Dye-sensitized solar cells (DSSCs), which can convert solar energy into electric energy by the photovoltaic effect, have been intensively studied as a promising candidate for the next-generation photovoltaic devices because of their simple structure, good stability, low manufacturing cost, and eco-friendly feature [1–5]. Over the past few years, although significant progress in DSSCs has been achieved, the power conversion efficiency (*PCE*) is still not satisfied compared to the silicon-based solar cells, which limits their further applications [6–8]. As is well known, the *PCE* of the DSSCs is strongly dependent on the light absorption ability of dyes such as N3, N-719, N-749, etc., which usually absorb energy from the relatively narrow sunlight spectrum in the visible wavelength range of 400–800 nm [3, 8]. Therefore, if the near-infrared (NIR) light (>800 nm) which comprises nearly 50 % in the sunlight could be converted into the visible light and reabsorbed by dyes, the *PCE* of DSSCs would be further improved.

Up to date, enormous methods have been carried out to improve the performances of solar cells, by incorporating with nanowire particles and upconverting materials [9–11]. In particular, the introduction of upconverting nanoparticles into DSSCs devices was considered as an alternative method to improve the efficiency of DSSCs. Since they can convert the low energy photons (NIR light) into the high energy ones (visible light), the enhanced solar energy generation of DSSCs can be obtained due to the increased visible light absorption in dyes [12–14]. Demopoulos et al. reported that the *PCE* enhancement by 10 % was achieved using β-$NaYF_4:Er^{3+}/Yb^{3+}$ nanoplatelets as the upconverting layer in DSSCs [13]. In addition, Wu et al. also showed the potential application of the Er^{3+}/Yb^{3+}-co-doped TiO_2 upconverting nanoparticles in DSSC, exhibiting a boosted *PCE* of 7.05 % (i.e., $PCE = 6.41$ % for the pristine DSSC)

* Correspondence: jsyu@khu.ac.kr
Department of Electronics and Radio Engineering, Kyung Hee University, Yongin 446-701, Republic of Korea

Springer

© 2015 Du et al. **Open Access** This article is distributed under the terms of the Creative Commons Attribution 4.0 International License (http://creativecommons.org/licenses/by/4.0/), which permits unrestricted use, distribution, and reproduction in any medium, provided you give appropriate credit to the original author(s) and the source, provide a link to the Creative Commons license, and indicate if changes were made.

[15]. Nevertheless, these obtained results are still far away from the practical application, so more efforts are required.

Recently, rare-earth (RE) ions doped nanomaterials were intensively investigated, and it was revealed that the luminescent properties of these RE ions doped nanomaterials can be modified by adjusting the size, shape, and phase of particles [16–18]. Among these nanomaterials, yttrium trioxide (Y_2O_3) is widely used as the optical host material owing to its high melting point, high thermal stability, and low toxicity [19, 20]. Furthermore, according to the Raman spectra, the Y_2O_3 has low phonon energy as low as ~600 cm^{-1} [21], which results in the high probability of the radiative transition. From this, it is expected that strong upconversion (UC) emissions could be obtained in RE ions doped Y_2O_3 material system. On the other hand, Er^{3+} ions, as a member of trivalent RE ions, have drawn considerable attention due to their unique green and red emissions corresponding to $(^2H_{11/2}, {}^4S_{3/2}) \rightarrow {}^4I_{15/2}$ and $^4F_{9/2} \rightarrow {}^4I_{15/2}$ transitions, respectively. Moreover, Yb^{3+} ions are usually co-doped with Er^{3+} ions, as a sensitizer, to improve the luminescent properties because of their strong absorption in the NIR wavelength region and efficient energy transfer (ET) from the Yb^{3+} to Er^{3+} ions [22]. Also, the light scattering properties can be affected by the nanoparticles with the size ranging from 200–1000 nm [2, 13]. In this work, the upconverting Er^{3+}/Yb^{3+}-co-doped Y_2O_3 (abbreviated as Y_2O_3:Er^{3+}/Yb^{3+}) nanoparticles were prepared by a urea-based homogeneous precipitation method and their structural and optical properties were investigated. After incorporating the Y_2O_3:Er^{3+}/Yb^{3+} into TiO_2 nanocrystalline films to form a composite photoelectrode in DSSCs, for the fabricated devices, the current density-voltage (*J-V*) characteristics and the incident photon to current conversion efficiency (*IPCE*) spectra were explored.

Methods

Sample Preparation

To obtain the optimum UC emission property [23], both the Er^{3+} and Yb^{3+} ion concentrations were fixed at 1 mol%, and the Y_2O_3:Er^{3+}/Yb^{3+} nanoparticles were successfully synthesized via a facile and simple urea-based homogeneous precipitation method, followed by appropriate thermal treatment. Briefly, stoichiometric amounts of yttrium nitrate hexahydrate ($Y(NO_3)_3 \cdot 6H_2O$, 99.8 %), erbium nitrate pentahydrate ($Er(NO_3)_3 \cdot 5H_2O$, 99.9 %), and ytterbium nitrate pentahydrate ($Yb(NO_3)_3 \cdot 5H_2O$, 99.9 %) were weighted and dissolved in 200 ml of deionized (DI) water to form a transparent solution. After that, moderate urea was added, and the mixed solution was sealed in a beaker, and then it was heated at 80 °C for 3 h under vigorous mechanical stirring. Subsequently, the precursor was centrifuged and washed with DI water and alcohol for several times to remove the remained ions. Finally, the precipitate was sintered at 800 °C for 3 h, thus, yielding the Y_2O_3:Er^{3+}/Yb^{3+} nanoparticles. For the fabrication of DSSCs, the cleaned fluorine doped tin oxide (FTO)-deposited glass substrates were used. Firstly, TiO_2 colloids (PST-18NR) were coated on the FTO surface to form a TiO_2 film with a thickness of ~5 μm by a doctor-blade method, and then the samples were sintered at 500 °C for 2 h. The TiO_2 colloids (PST-400C) mixed with 1 wt% Y_2O_3:Er^{3+}/Yb^{3+} nanoparticles were subsequently screen-printed on the TiO_2 film, which creates a 5-μm-thick TiO_2 + Y_2O_3:Er^{3+}/Yb^{3+} layer. Afterwards, the as-prepared film was soaked in the N-719 dye solution (3×10^{-4}M in ethanol) for 24 h. For comparison, a dye-sensitized TiO_2 film without Y_2O_3:Er^{3+}/Yb^{3+} nanoparticles was also prepared. Meanwhile, the platinum (Pt) counter electrode was prepared on the FTO glass using Pt paste (Dyesol, counter PT-1), followed by heating at 500 °C for 2 h. Lastly, the DSSC devices were assembled by an injection of electrolyte (Dyesol, electrolyte HPE) and a sealing process with the help of a hot press.

Characterization

The phase structure of the fabricated nanophosphor samples was analyzed by using an X-ray diffractometer (XRD; Mac Science, M18XHF-SRA) with Cu Kα (λ = 1.5402 Å) radiation, and the JADE software was applied to analyze the XRD data. The structural morphology was observed by using a transmission electron microscope (TEM; JEM-2100 F, JEOL). The room-temperature UC spectrum was checked by using a fluorescence spectrophotometer (Ocean optics USB 4000) under the excitation of a laser light at a wavelength (λ) of 980 nm with a pump power of 660 mW. The optical transmission and reflection spectra of dye-sensitized photoanodes with and without Y_2O_3:Er^{3+}/Yb^{3+} phosphor nanoparticles were characterized by using a UV–vis-NIR spectrophotometer (Cary 5000, Varian). The J-V curves were measured by using a photocurrent system consisting of a solar simulator (ABET, SUN 3000) with a 1000 W Xe short-arc lamp and a source meter (Keithley 2400). The *IPCE* spectra from 300 to 800 nm were evaluated by using a 300 W xenon arc lamp as the light source coupled to a monochromator (TLS-300× xenon light source, Newport) with an optical power meter (2935-c, Newport).

Results and Discussion

From the XRD pattern in Fig. 1a, it was observed that the diffraction peaks were consistent with the standard pattern (JCPDS#41-1105) and no impurity phases were detected. This means that the powders with a pure cubic phase of Y_2O_3 were synthesized and the RE (Er^{3+}, Yb^{3+}) ions were well diffused into the Y_2O_3 host lattice. In

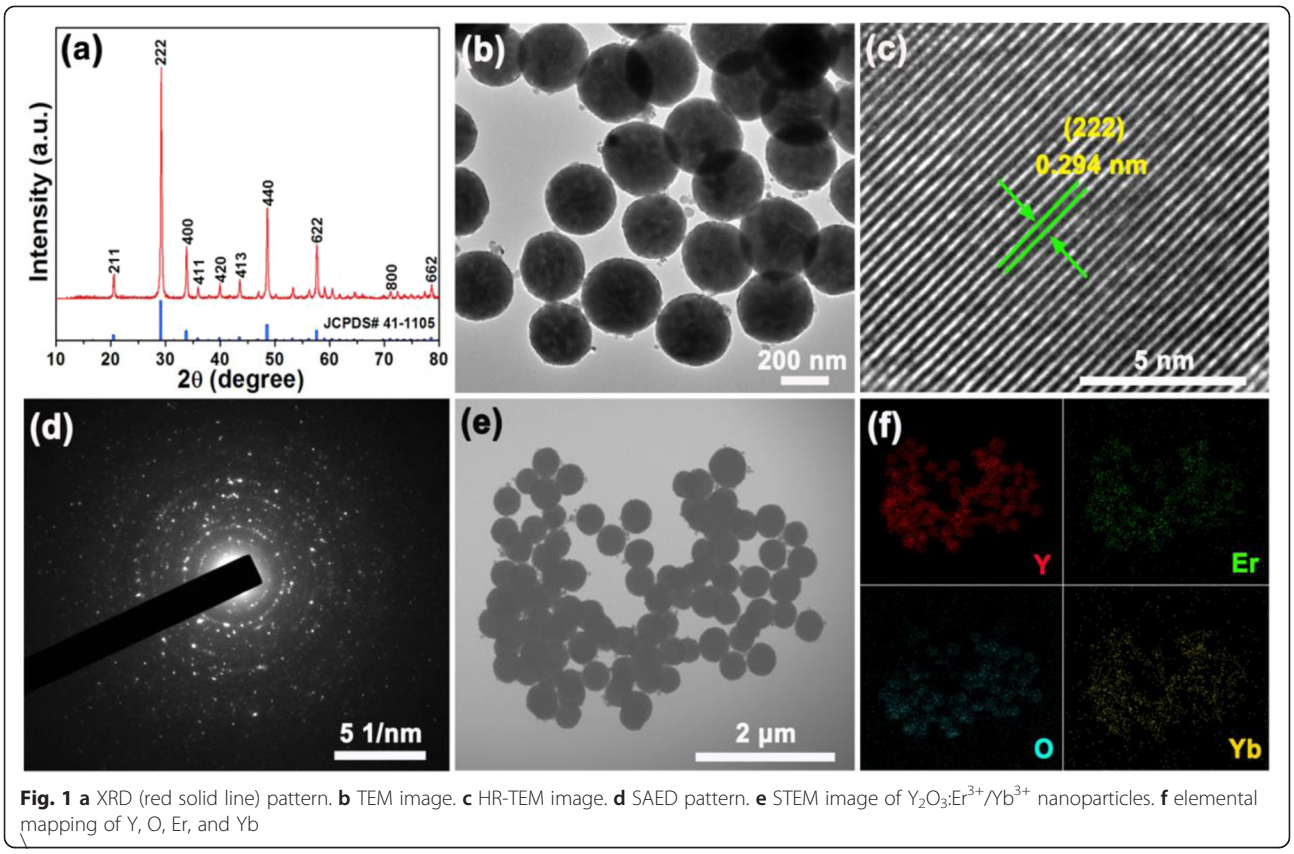

Fig. 1 **a** XRD (red solid line) pattern. **b** TEM image. **c** HR-TEM image. **d** SAED pattern. **e** STEM image of Y_2O_3:Er^{3+}/Yb^{3+} nanoparticles. **f** elemental mapping of Y, O, Er, and Yb

Fig. 1b, the TEM image confirmed that the as-prepared Y_2O_3:Er^{3+}/Yb^{3+} nanoparticles have sphere-like morphologies with the size range of 250–300 nm which is larger than those of the sample prepared by a coprecipitation method (70 nm) [23]. Furthermore, from the high-resolution TEM (HR-TEM) image in Fig. 1c, the interplanar distance between the adjacent lattice planes was estimated to be about 0.294 nm, which is well matched with the (222) plane of the Y_2O_3. In Fig. 1d, the selected area electron diffraction (SAED) pattern displayed bright dots and rings. This indicates that the samples are relatively well crystallized. As shown in Fig. 1f, the elemental mapping image taken from the area in the scanning transmission electron microscope (STEM) image of Fig. 1e demonstrates that the constituent materials of Y, O, Er, and Yb are uniformly distributed.

Figure 2a, depicts the UC emission spectrum of the Y_2O_3:Er^{3+}/Yb^{3+} nanoparticles. Under the light excitation at $\lambda_{ex} = 980$ nm, the fabricated samples exhibited a strong yellow UC emission that can be seen by the naked eye as shown in the inset of Fig. 2a. As shown in Fig. 2a, it is clear that the UC spectrum consists of three distinct bands, that is, two green emissions at $\lambda = 510$–542 nm and 542–570 nm and strong red emission at $\lambda =$ 625–700 nm. The former is attributed to the $^2H_{11/2} \rightarrow {}^4I_{15/2}$ and $^4S_{3/2} \rightarrow {}^4I_{15/2}$ transitions, respectively and the latter is ascribed to the $^4F_{9/2} \rightarrow {}^4I_{15/2}$ transition [19, 24]. These results give a reasonable agreement with the previous reports on Er^{3+}-doped materials [22, 25]. Here, it is noteworthy that these emission bands are located in the absorption wavelength range of the N-719 dye (i.e., $\lambda =$ 300–800 nm). Thus, the use of Y_2O_3:Er^{3+}/Yb^{3+} nanoparticles in N-719 dye-based photovoltaic devices would increase the photocurrents due to the enhanced light absorption, except for the sunlight, caused by their green and red light emissions converted from the lights at NIR wavelengths, and thus, the improved device performance of DSSCs could be achieved.

The energy level diagram of Er^{3+} and Yb^{3+} ions including possible UC processes is illustrated in Fig. 2b. Under the light excitation at $\lambda_{ex} = 980$ nm, the Yb^{3+} ions are excited from the ground sate to the $^2F_{5/2}$ level and they drop back. Thus, the energy is transferred to the adjacent Er^{3+} ions, resulting in the population of $^4I_{11/2}$ level. Then, the multiphonon relaxation (MPR) process occurs, and part of the $^4I_{11/2}$ level decays to the $^4I_{13/2}$ level. Meanwhile, the Yb^{3+} ions absorb the second photon energy, and again, the energy is transferred to the adjacent Er^{3+} ions, and the $^4F_{9/2}$ and $^4F_{7/2}$ levels are populated. Subsequently, the electrons relax to the $^2H_{11/2}$, $^4S_{3/2}$, and $^4F_{9/2}$ levels due to the non-radiative (NR) process. As a result, the strong green and red UC emissions are

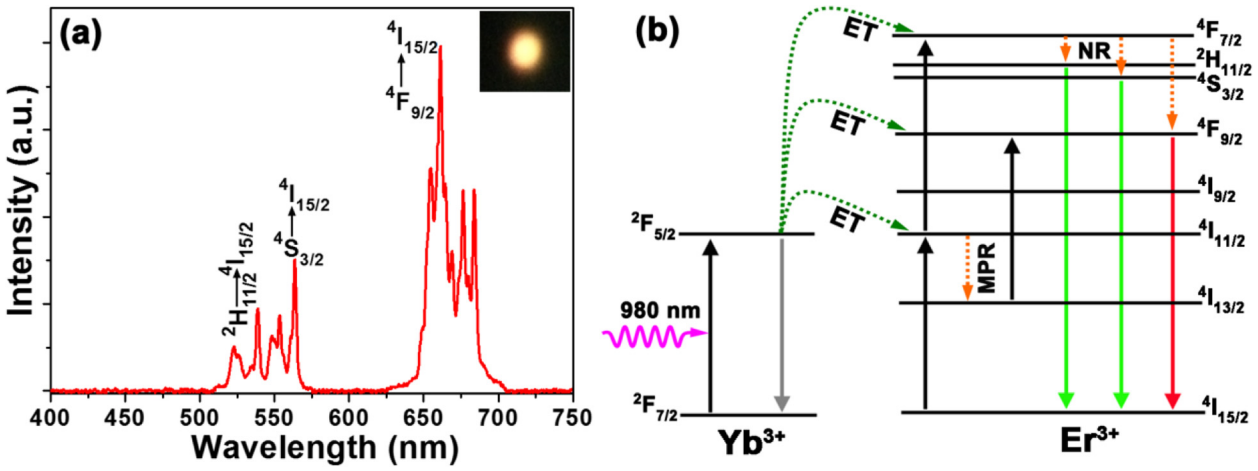

Fig. 2 a UC spectrum of $Y_2O_3:Er^{3+}/Yb^{3+}$ nanoparticles (red solid line) under 980 nm light excitation and **b** schematic energy level diagram of Yb^{3+} and Er^{3+} ions and proposed UC mechanism in $Y_2O_3:Er^{3+}/Yb^{3+}$ nanoparticles under 980 nm light excitation. The inset of **a** shows the photograph taken in the darkness by using a digital camera

observed due to the $^2H_{11/2} \rightarrow {}^4I_{15/2}$, $^4S_{3/2} \rightarrow {}^4I_{15/2}$ and $^4F_{9/2} \rightarrow {}^4I_{15/2}$ transitions, respectively.

To investigate the light-scattering behaviors of the $Y_2O_3:Er^{3+}/Yb^{3+}$ nanoparticles in DSSCs, the absorption (i.e., 1-*R*-*T*) of the dye-sensitized photoanodes with the $Y_2O_3:Er^{3+}/Yb^{3+}$ nanoparticles was extracted by the measured total reflection (*R*) and transmission (*T*) spectra in Fig. 3. As can be seen in Fig. 3a, there were differences in both the total transmission and reflection between the dye-sensitized photoanodes consisting of the TiO_2 and the $TiO_2 + Y_2O_3:Er^{3+}/Yb^{3+}$. Especially, the transmission was further decreased. From these results, as shown in the absorption spectra of Fig. 3b, it can be observed that the dye-sensitized photoanode consisting of the $TiO_2 + Y_2O_3:Er^{3+}/Yb^{3+}$ exhibited the relatively higher absorption spectrum compared to one consisting of only TiO_2 over a wide wavelength region of 350–750 nm. This indicates the enhancement of the light-scattering property in the dye-sensitized photoelectrodes by incorporating the $Y_2O_3:Er^{3+}/Yb^{3+}$ nanoparticles into the TiO_2 photoelectrode, and thus, it can lead to the higher photocurrents in DSSCs due to the enhancement in light absorption.

To investigate the influence of the UC emission phosphors on the photovoltaic performance of DSSCs, the $Y_2O_3:Er^{3+}/Yb^{3+}$ nanoparticles were introduced into the TiO_2 photoelectrode. Figure 4 shows (a) the *J-V* curves and (b) the *IPCE* spectra of the DSSCs with and without the $Y_2O_3:Er^{3+}/Yb^{3+}$ nanoparticles. The device characteristics (i.e., short-circuit current density; J_{SC}, open-circuit voltage; V_{OC}, fill factor; *FF*, *PCE*)

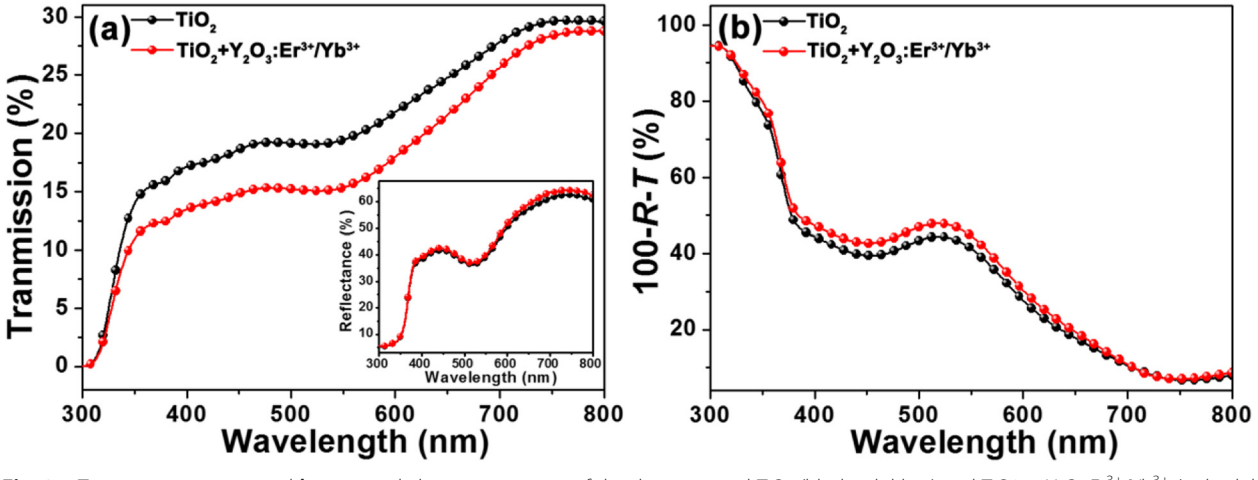

Fig. 3 a Transmission spectra and **b** estimated absorption spectra of the dye-sensitized TiO_2 (black solid line) and TiO2 + $Y_2O_3:Er^{3+}/Yb^{3+}$ (red solid line) photoelectrodes. The inset of **a** shows the reflectance spectra of the corresponding samples

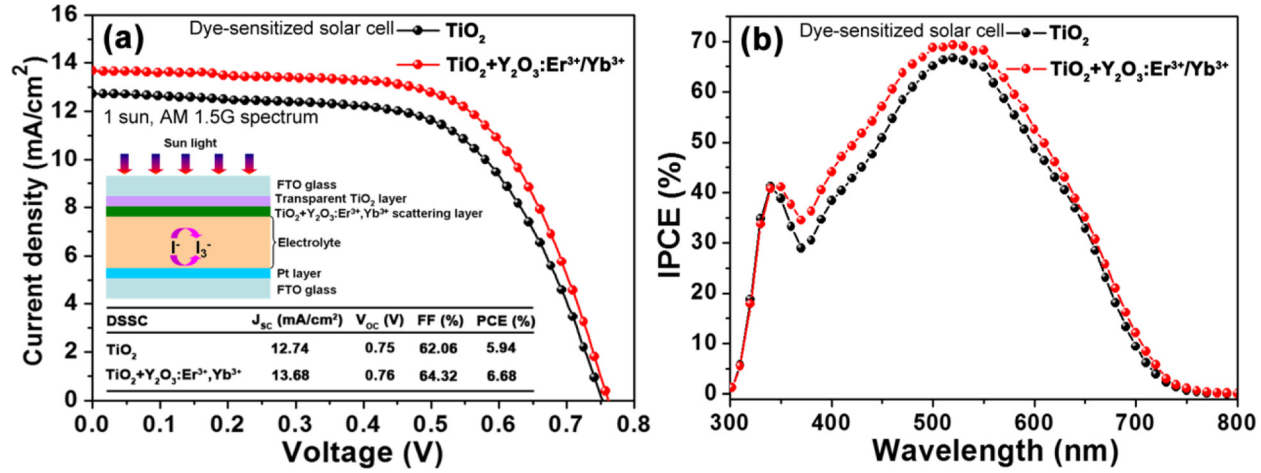

Fig. 4 **a** *J-V* curves and **b** IPCE spectra of the DSSCs with (red solid line) and without (black solid line) $Y_2O_3:Er^{3+}/Yb^{3+}$ nanoparticles (1 wt%). The inset of **a** shows the schematic diagram of the DSSC with $Y_2O_3:Er^{3+}/Yb^{3+}$ nanoparticles and its photovoltaic performance parameters

of the corresponding DSSC devices are summarized in the inset of Fig. 4a. The corresponding schematic diagram of the DSSC with the $Y_2O_3:Er^{3+}/Yb^{3+}$ nanoparticles is also shown. As shown in Fig. 4a, the DSSC without the $Y_2O_3:Er^{3+}/Yb^{3+}$ nanoparticles exhibited the photovoltaic characteristics of $J_{SC} = 12.74$ mA/cm^2, $V_{OC} =$ 0.75 V, $FF = 62.06$ % and $PCE = 5.94$ %. In contrast, by employing the $Y_2O_3:Er^{3+}/Yb^{3+}$ nanoparticles in the DSSC, for all the photovoltaic characteristics, the increased values of $J_{SC} = 13.68$ mA/cm^2, $V_{OC} = 0.76$ V, FF = 64.32 %, and $PCE = 6.68$ % were measured, which leads to the significant *PCE* increment ratio of ~12.4 %. This is mainly because a considerable enhancement (i.e., increment ratio of ~7.4 %) in the J_{SC} is caused by the efficient UC emissions of Er^{3+} ions from the NIR light to the visible light as well as the enhanced light-scattering properties [26, 27]. The V_{OC} also increased slightly. According to previous reports [27, 28], the V_{OC} corresponds to the energy difference between the electronic Fermi level of TiO_2 film and the redox potential of I^-/I_3^-, i.e., $V_{OC} = E_{F(TiO2)} - E_{redox}$. It is well known that when RE ions are doped and substituted into the Ti^{4+} sites in the TiO_2, a p-type doping effect appears, resulting in the increment of the Fermi level of the TiO_2 [29]. Thus, the V_{OC} was enhanced. Using the $Y_2O_3:Er^{3+}/Yb^{3+}$ nanoparticles, the increased photocurrents by the light-scattering effect can be also verified by the *IPCE* data. As can be seen in Fig. 4b, the DSSC with the $Y_2O_3:Er^{3+}/Yb^{3+}$ nanoparticles showed a higher IPCE spectrum compared to the DSSC without $Y_2O_3:Er^{3+}/Yb^{3+}$ nanoparticles over an entire spectra range of 350–750 nm. This is well matched with the aforementioned absorption properties in Fig. 3b.

Conclusions

In summary, the upconverting $Y_2O_3:Er^{3+}/Yb^{3+}$ phosphor nanoparticles were synthesized and introduced into the TiO_2 photoelectrode of DSSCs. Under the excitation of the NIR ($\lambda_{ex} = 980$ nm) light, the strong green and red UC emissions, corresponding to the ($^2H_{11/2}$, $^4S_{3/2}$) $\rightarrow$ $^4I_{15/2}$ and $^4F_{9/2} \rightarrow {}^4I_{15/2}$ transitions, respectively, were observed with the light-scattering effect over a wide wavelength range of 350–750 nm. For the DSCCs incorporated with the $Y_2O_3:Er^{3+}/Yb^{3+}$ nanoparticles, the enhanced photovoltaic performance was achieved, indicating the increase in the *PCE* value from 5.94 to 6.68 % (i.e., *PCE* increment ratio of ~12.4 %). These results can provide a better insight into the phosphor nanoparticles with the NIR sunlight-upconverting functions into the visible lights as well as the light-scattering effect for high-performance dye-sensitized photovoltaic devices.

Competing interests

The authors declare that they have no competing interests.

Authors' contributions

PD prepared and characterized the nanoparticles. JHL and SMC synthesized the DSSCs devices. PD and JSY cowrote the manuscript. JWL participated in revising the manuscript. All authors read and approved the final manuscript.

Acknowledgements

This work was supported by the National Research Foundation of Korea (NRF) grant funded by the Korea government (MSIP) (No. 2014–069441).

Received: 8 July 2015 Accepted: 30 July 2015
Published online: 12 August 2015

References

1. O'Regan B, Grätzel M. A low-cost, high-efficiency solar cell based on dye-sensitized colloidal TiO_2 films. Nature. 1991;353:737–40.

2. Kawamura G, Ohmi H, Tan WK, Lockman Z, Muto H, Matsuda A. Ag nanoparticle-deposited TiO_2 nanotube arrays for electrodes of dye-sensitized solar cells. Nanoscale Res Lett. 2015;10:219.
3. Liang L, Liu Y, Bu C, Guo K, Sun W, Huang N. Highly uniform, bifunctional core/double-shell-structured β-$NaYF_4$:Er^{3+}, Yb^{3+} @SiO_2@TiO_2 hexagonal sub-microprisms for high-performance dye sensitized solar cell. Adv Mater. 2013;25:2174–80.
4. Zhou Z, Wang J, Nan F, Bu C, Yu Z, Liu W, et al. Upconversion induced enhancement of dye sensitized solar cell based on core-shell structured β-$NaYF_4$:Er^{3+}, Yb^{3+}@SiO_2 nanoparticles. Nanoscale. 2014;6:20525–5055.
5. Huang X, Han S, Huang W, Liu X. Enhancing solar cell efficiency: the search for luminescent materials as spectral converters. Chem Soc Rev. 2013;42:173–201.
6. Shan G, Demopoulos GP. Near-infrared sunlight harvesting in dye-sensitized solar cells via the insertion of an upconverter-TiO_2 nanocomposite layer. Adv Mater. 2010;22:4373–7.
7. Yuan C, Chen G, Li L, Damasco JA, Ning Z, Xing H, et al. Simultaneous multiple wavelength upconversion in a core-shell nanoparticle for enhanced near infrared light harvesting in a dye-sensitized solar cell. ACS Appl Mater Interfaces. 2014;6:18018–25.
8. Ramasamy P, Kim J. Combined plasmonic and upconversion rear reflector for efficient dye-efficient dye-sensitized solar cells. Chem Commun. 2014;50:879–81.
9. Chen C, Ban D, Helander MG, Lu ZH, Poole P. Near-infrared inorganic/organic optical upvonverter with an external power efficiency of >100%. Adv Mater. 2010;22:4900–4.
10. Ko SH, Lee D, Kang HW, Nam KH, Yeo JY, Hong SJ, et al. Nanoforest of hydrothermally grown hierarchical ZnO nanowires for a high efficiency dye-sensitized solar cell. Nano Lett. 2011;11:666–71.
11. Wang X, Yan X. Ultraviolet and infrared photo-excited synergistic effect in Er^{3+}-doped YbF_4 phosphors. Opt Lett. 2011;36:4353–5.
12. Ramasamy P, Manivasakan P, Kim J. Upconversion nanophosphors for solar cell applications. RSC Adv. 2014;4:34873–95.
13. Shan GB, Assaaoudi H, Demopoulos G. Enhanced performance of dye-sensitized solar cells by utilization of an external, bifunctional layer consisting of uniform β-$NaYF_4$:Er^{3+}/Yb^{3+} nanoplatelets. ACS Appl Mater Interfaces. 2011;3:3239–43.
14. Liang L, Liu Y, Zhao X. Double-shell β-$NaYF_4$:Yb^{3+}, Er^{3+}/SiO_2/TiO_2 submicroplates as a scattering and upconverting layer for efficient dye-sensitized solar cell". Chem Commum. 2013;49:958–3960.
15. Xie G, Wei Y, Fan L, Wu J. Application of doped rare-earth doped oxide TiO_2:(Tm^{3+}, Yb^{3+}) in dye-sensitized solar cell. J Phys Conf Ser. 2012;339:012010.
16. Feng X, Sayle DC, Wang ZL, Paras MS, Santora B, Sutorik AC, et al. Converting ceria polyhedral nanoparticles into single-crystal nanospheres. Science. 2006;312:1504–8.
17. Wang X, Bu Y, Xiao Y, Kan C, Lu D, Yan X. Size and shape modifications, phase transition, and enhanced luminescence of fluoride nanocrystals induced by doping. J Mater Chem C. 2013;1:3158–66.
18. Yang L, Li Y, Yu S, Hao J, Zhong J, Chu PK. Phase transformation and size tuning in controlled-growth of nanocrystals via self-seeded nucleation with preferential thermodynamic stability. Chem Commun. 2011;47:12544–6.
19. Du P, Luo L, Yue Q, Li W. The simultaneous realization of high- and low-temperature thermometry in Er^{3+}/Yb^{3+}-co-doped Y_2O_3 nanoparticles. Mater Lett. 2015;143:209–11.
20. Wu J, Xie G, Lin J, Lan Z, Huang M, Huang Y. Enhancing photoelectrical performance of dye-sensitized solar cell by doping with europium-doped yttria rare-earth oxide. J Power Sources. 2010;195:6937–40.
21. Abrashev MV, Todorov ND, Geshev J. Raman spectra of R_2O_3 (R-rare-earth) sesquioxides with C-type bixbytie crystal structure: a comparative study. J Appl Phys. 2014;116:103508.
22. Du P, Yu JS. Effect of molybdenum on upconversion emission and temperature sensing properties in $Na_{0.5}Bi_{0.5}TiO_3$:Er/Yb ceramics. Ceram Int. 2015;41:6710–4.
23. Lu P, Hou Y, Tang A, Wu H, Teng F. Upconversion multicolor tuning: red to green emission from Y_2O_3:Er, Yb nanoparticles by calcination. Appl Phys Lett. 2013;102:233103.
24. Zhou N, Qiu P, Wang K, Fu H, Gao G, He R, et al. Shape-controllable synthesis of hydrophilic $NaLuF_4$:Yb, Er nanocrystals by a surfactant-assistant two-phase system. Nanoscale Res Lett. 2013;8:518.
25. Lojpur VM, Ahrenkiel PS. Dramićanin: color-tunable up-conversion emission in Y_2O_3:Yb^{3+}, Er^{3+} nanoparticles prepared by polymer complex solution method. Nanoscale Res Lett. 2013;8:131.
26. Zou Z, Wang J, Nan F, Bu C, Yu Z, Liu W, et al. Upconversion induced enhancement of dye sensitized solar cells based on core-shell structured β-$NaYF_4$:Yb^{3+}/Er^{3+}@SiO_2 nanoparticles. Nanoscale. 2014;6:20525–2055.
27. Wang J, Wu J, Lin J, Huang M, Huang Y, Lan Z, et al. Application of Y_2O_3:Er^{3+} nanorods in dye-sensitized solar cells. ChemSusChem. 2012;5:1307–12.
28. Grätzel M. Photoelectrochemical cells. Nature. 2001;414:338–44.
29. Schlichthörl G, Huang SY, Sprague J, Frank AJ. Band edge movement and recombination kinetics in dye-sensitized nanocrystalline TiO_2 solar cell: a study by intensity modulated photovoltage spectroscopy. J Phys Chem B. 1997;101:8141–55.

Submit your manuscript to a SpringerOpen journal and benefit from:

- ► Convenient online submission
- ► Rigorous peer review
- ► Immediate publication on acceptance
- ► Open access: articles freely available online
- ► High visibility within the field
- ► Retaining the copyright to your article

Submit your next manuscript at ► springeropen.com